Hydrol. Earth Syst. Sci. Discuss., 6, 2337–2365, 2009
www.hydrol-earth-syst-sci-discuss.net/6/2337/2009/

Hydrology and Earth System Sciences Discussions

Papers published in *Hydrology and Earth System Sciences Discussions* are under open-access review for the journal *Hydrology and Earth System Sciences*

A Bayesian approach to estimate sensible and latent heat over vegetation

C. van der Tol[1], S. van der Tol[2], A. Verhoef[3], B. Su[1], J. Timmermans[1], C. Houldcroft[3], and A. Gieske[1]

[1]ITC International Institute for Geo-Information Science and Earth Observation, Hengelosestraat 99, P.O. Box 6, 7500 AA Enschede, The Netherlands
[2]Delft University of Technology, Faculty of Electrical Engineering, Mekelweg 4, 2628 CD Delft, The Netherlands
[3]The University of Reading, Department of Soil Science, School of Human and Environmental Sciences, Reading RG6 6DW, UK

Received: 29 January 2009 – Accepted: 7 February 2009 – Published: 16 March 2009

Correspondence to: C. van der Tol (tol@itc.nl)

Published by Copernicus Publications on behalf of the European Geosciences Union.

Abstract

Sensible and latent heat fluxes are often calculated from bulk transfer equations combined with the energy balance. For spatial estimates of these fluxes, a combination of remotely sensed and standard meteorological data from weather stations on the ground is used. The success of this approach depends on the accuracy of the input data and on the accuracy of two variables in particular: aerodynamic and surface conductance. This paper presents a Bayesian approach to improve estimates of sensible and latent heat fluxes by using a priori estimates of aerodynamic and surface conductance alongside remote measurements of surface temperature. The method is validated for time series of half-hourly measurements in a fully grown maize field, a vineyard and a forest. It is shown that the Bayesian approach yields more accurate estimates of sensible and latent heat flux than traditional methods.

1 Introduction

Sensible, H, and latent heat (i.e. evapotranspiration), λE, fluxes between the land surface and atmosphere are important components of the Earth's surface energy balance (see Eq. 1). Different techniques exist to estimate them, generally based on micrometeorological methods, including the eddy-covariance, Bowen ratio technique and bulk transfer equations (see Eqs. 2 and 3), for example. Alternatively, estimates of evapotranspiration can be obtained from the soil water balance (see e.g. Verhoef and Campbell, 2005, for an overview of both types of methods), from which sensible heat flux could be derived, if values of net radiation and soil heat flux were available (see Eq. 1).

Field scale measurements are used to study the local water and energy balance and to gain process understanding, but they are often not representative for large areas. Remote sensing measurements provide a spatial coverage, but not all variables needed to estimate sensible and latent heat can be measured by remote sensing.

It is common practice to combine remote sensing and field data to estimate H and

λE spatially (e.g. Su, 2002). Latent heat flux is either solved as a residual term in the energy balance, with H obtained from a bulk transfer equation (see Eq. 2) or directly calculated using the bulk transfer equation for latent heat flux. The problem with the latter approach, however, is that estimates of specific humidity at the land surface are hard to obtain.

Remote sensing products used as input include brightness temperature and emissivity (Bastiaanssen et al., 1998), reflected shortwave radiation and NDVI, which are used for the derivation of vegetation structure and aerodynamic resistance (Su, 2002). Weather station variables include wind speed, air temperature and humidity.

There are various sources of uncertainty associated with these estimates: the representativeness of the weather station data, the atmospheric correction of satellite data, the derivation of remote sensing products, the relationship between remote sensing products and surface characteristics (such as aerodynamic resistance), the model itself, and the interpolation in time between satellite overpasses. Aerodynamic and surface resistances are particularly difficult to estimate.

Nowadays hydrologists often use data assimilation techniques to handle uncertainties in parameters and (satellite) observations (Troch et al., 2003). Schuurmans et al. (2003) used remote sensing estimates of λE to improve the predictions of a hydrological model. Posterior estimates of λE were calculated as a weighted mean of a traditional, ground based method (the Makkink method) and a remote sensing method (SEBAL, Bastiaanssen et al., 1998). Crow and Wood (2003), by using an ensemble Kalman filter (EnKF), were able to retrieve spatial and temporal trends in root water extraction by vegetation from observations of surface temperature and ancillary data. EnKFs are also common practice in the retrieval of soil moisture from microwave remote sensing (among others, Reichle et al., 2002).

Franks et al. (1999) indicated that land surface temperature measurements may serve to constrain the parameter space in Soil-Vegetation-Atmosphere-Transfer (SVAT) models, thus leading to better estimates of sensible and latent heat fluxes. This paper presents a Bayesian approach in which a priori information about two key SVAT variables (aerodynamic and surface resistance) is used beside measurements of surface temperature in order to improve estimates of sensible and latent heat. We have purposely chosen for the simplest SVAT model and the simplest data assimilation approach, such that the implementation in any ground-based and remote sensing-based SVAT model is straightforward. For longer time series or for pixel by pixel calculations, the model can be transformed into a Kalman filter (KF) or EnKF.

In this paper, the method is applied to data measured at field scale during field campaigns. Time series of weather data and infrared radiometer measurements from three land cover types are used: a maize field, a vineyard and a forest. Although no remote sensing data are used, we used proximal observations of surface temperature and therefore the approach can be applied to a combination of field and satellite data in a similar way. It will be shown that the Bayesian approach, using both a priori information and measurements, results in more accurate estimates of sensible and latent heat then using only either a priori information or measurements.

2 Theory

2.1 Energy balance

A simple energy balance equation is used, consisting of four components: net radiation received by the surface, R_n, soil heat flux, G, sensible heat flux, H and latent heat flux, λE (all in $\mathrm{W\,m^{-2}}$). Energy involved in melting and freezing or in chemical reactions, energy stored in the canopy, and energy horizontally transported by advection are ignored. Hence:

$$R_n - G = H + \lambda E \tag{1}$$

Parameter λ is the latent heat of evaporation of water ($\mathrm{J\,kg^{-1}}$) and E the evapotranspiration rate ($\mathrm{kg\,m^{-2}\,s^{-1}}$).

Sensible and latent heat flux are the fluxes of heat and water vapour between the surface and the atmosphere carried by turbulent air flow. They are calculated as the product of a conductance and a driving force between the surface (subscript "s") and the air at measurement height (subscript "a"):

$$H = \rho c_p g_a (T_s - T_a) \tag{2}$$

$$\lambda E = \lambda \frac{1}{1/g_a + 1/g_s} (q_s(T_s) - q_a) \tag{3}$$

where ρ is the mass density of air (kg m^{-3}), c_p the heat capacity of air (J kg^{-1} K^{-1}), g_a is the aerodynamic conductance (m s^{-1}) for transport of heat and vapour from the surface boundary layer into the atmosphere, g_s is the surface conductance for water vapour transport from stomatal cavities in leaves or soil pores to the leaf or soil surface boundary layer (m s^{-1}), T_s is surface temperature and T_a is air temperature (both in K), q_s is the vapour concentration in stomata or soil pores (kg m^{-3}), and q_a is the vapour concentration in the air (kg m^{-3}).

The model consists of three equations with ten unknowns (Table 1, ρs c_p and λ are considered constants). Usually, seven of them are measured or estimated, and the remaining three calculated. In most approaches, H, λE and T_s are unknown, while the other variables are known. In the Penman-Monteith approach, H and T_s are eliminated and an approximation for $q_s(T_s)$ is used, resulting in one equation with seven unknowns.

Surface conductance of individual leaves can be derived from leaf gas exchange measurements, but scaling to canopy level is not trivial (Baldocchi et al., 1991). Stomatal regulation is a function of actual photosynthesis rate, soil moisture content, air humidity, air temperature and the species composition of the vegetation. At canopy level, empirical and semi-empirical relationships between surface conductance and environmental conditions are commonly used (Jarvis, 1976; Cowan, 1977; Ball et al., 1987; Leuning, 1995). These relationships require vegetation-specific, a priori coefficients or local calibration against measured fluxes of water and carbon dioxide. However, for many applications these models are too detailed, as parameters for the vegetation under study are often not available.

The aerodynamic conductance g_a depends on the momentum and scalar roughness length of the surface, z_{0M} (m) and z_{0H} (m), respectively, wind speed u (m s^{-1}), and stability of the atmosphere, as combined in the logarithmic wind profile (Tennekes, 1973; Garratt, 1992). The momentum roughness length, z_{0M}, is usually estimated from leaf area index and vegetation height (e.g. Raupach 1994; Verhoef et al., 1997a), the scalar roughness length, z_{0H}, is often taken as a constant fraction of z_{0M}, although it varies widely, largely depending on canopy density (Stewart et al., 1994; Verhoef et al, 1997b). Optical remote sensing is often used to estimate vegetation height and leaf area index (Su, 2002). However, estimates of aerodynamic resistance based on optical remote sensing contain a large degree of uncertainty.

2.2 Classic approaches

The difficulty in estimating g_a and g_s in Eqs. (1–3) has been overcome in a number of ways. This has resulted in three techniques to calculate evapotranspiration from the energy balance:

1. FAO-approach: evapotranspiration is calculated by multiplying a "reference evapotranspiration" by an empirical coefficient for a specific crop, extracted from an expert knowledge based table. The reference evapotranspiration is calculated for a crop with known values for g_a and g_s, usually the typical short, well-watered grass of a meteorological station. This method is disseminated by the FAO (Allen et al., 1998, 2006), and is mainly used to calculate irrigation requirements.

2. T_s-approach: evapotranspiration is calculated by solving Eqs. (1–3) with H, λE and g_s as unknowns. In that case, on top of the standard meteorological variables, surface temperature measurements and estimates of aerodynamic conductance g_a are required. This technique is used in remote sensing, for example in the

model SEBS (Su, 2002). Surface temperature is retrieved from thermal remote sensing, and aerodynamic resistance from optical remote sensing.

3. A priori approach: evapotranspiration is calculated by solving Eqs. (1–3) with H, λE and T_s as unknowns. Aerodynamic conductance is estimated from a measured wind profile or from a priori values for a specific vegetation type, and surface conductance g_s is estimated with one of the combined photosynthesis-conductance or empirical models discussed above. Values for the parameters of such model are found from calibration of the model against measurements of g_s or taken from the literature.

The use of surface temperature in the T_s-approach introduces another source of uncertainty. Sensible heat flux is proportional to $T_s - T_a$, a relatively small difference between two measurements. As a result, the error in H will be relatively large compared to the errors in T_a and T_s, especially when T_s is taken from remote sensing and T_a from weather station data.

2.3 Bayesian approach

The aim of the Bayesian approach proposed in this paper is to combine the approaches (2) and (3). None of the variables g_s, g_a and T_s is considered as unknown, but a priori information about g_s, g_a and measurements of T_s are used to calculate the least square error posterior estimates of g_s, g_a and T_s (and thus also of H and λE). The use of a priori values avoids unrealistic values for g_s, g_a, and the use of measurements prevents unrealistic values of T_s. It is expected that more realistic values for g_s, g_a and T_s also lead to improved estimates of H and λE.

The model (Eqs. 1–3) is re-written such that T_s is output of the model, by eliminating H and λE from Eqs. (1–3) and writing T_s as the dependent variable. In other words, T_s is a function of all input variables and parameters. Hence:

$$\tilde{\boldsymbol{x}} = f(\boldsymbol{\theta}) + \boldsymbol{w} \tag{4}$$

where $\tilde{\boldsymbol{x}}$ represents the measured output (in this case measured T_s, the squiggly symbol is used to denote a measurement), f the model equations, $\boldsymbol{\theta}$ a vector of variables and parameters , and $\boldsymbol{w}$ background noise caused by the uncertainty of the model and measurements. The vector notation is used if the problem is solved for multiple time steps, multiple pixels, or for multiple measurements and parameters. This aspect is discussed later in this paper.

A priori estimates of surface and aerodynamic conductance, and measurements of surface temperature are used to calculate posterior values. Parameter values have a probability density function of $p(\boldsymbol{\theta})$, and measurements a probability density function of $p(\tilde{\boldsymbol{x}}|\boldsymbol{\theta})$. The posterior probability density of the parameters (i.e. the parameter values given the measurements of T_s), is calculated with the classic Bayes' theorem:

$$p(\boldsymbol{\theta}|\tilde{\boldsymbol{x}}) = \frac{p(\tilde{\boldsymbol{x}}|\boldsymbol{\theta}) \cdot p(\boldsymbol{\theta})}{\int p(\tilde{\boldsymbol{x}}|\boldsymbol{\theta}) \cdot p(\boldsymbol{\theta}) d\boldsymbol{\theta}} \tag{5}$$

The minimum least square error estimate of the parameters, given the measurements, is the expected value of the parameters. The expected value can be calculated as:

$$\boldsymbol{\theta} = E(\boldsymbol{\theta}|\tilde{\boldsymbol{x}}) = \int \boldsymbol{\theta} \cdot p(\boldsymbol{\theta}|\tilde{\boldsymbol{x}}) d\boldsymbol{\theta} \tag{6}$$

The integration in Eq. (6) is avoided by calculating only the peak of the probability density function:

$$\widehat{\boldsymbol{\theta}} = \arg\max_{\underline{\theta}} p(\boldsymbol{\theta}\,|\tilde{\boldsymbol{x}}) = \arg\min_{\underline{\theta}} \left(\left| C_x^{-1/2} \left(f(\boldsymbol{\theta}) - \tilde{\boldsymbol{x}} \right) \right|^2 + \left| C_\theta^{-1/2} (\boldsymbol{\theta} - \boldsymbol{\theta}_0) \right|^2 \right) \tag{7}$$

where C_x and C_θ are the covariance matrices for the measurements and the parameters, respectively. Parameters $\widehat{\boldsymbol{\theta}}$ are the posterior parameters used later to calculate sensible and latent heat flux.

HESSD

6, 2337–2365, 2009

A Bayesian approach to estimate sensible and latent heat over vegetation

C. van der Tol et al.

The last part of Eq. (7) between the brackets is a cost function or the quadratic error. The quadratic error is the sum of the quadratic error in the parameters (θ) scaled with the uncertainty of the a priori estimates, and the quadratic error in the measurements of T_s, scaled with the uncertainty of the measurements of T_s. The optimum parameter values are located at the minimum error. If both $p(\tilde{\boldsymbol{x}}\|\boldsymbol{\theta})$ and $p(\boldsymbol{\theta})$ are Gaussian, then the solution is exact (and Eqs. 6 and 7 will give equal results), otherwise it is an approximation. In this study, Gaussian distributions for both functions are assumed.

The key issues are to estimate a priori values of θ, and to estimate the two covariance matrices. These matrices describe the uncertainty of all input (measurements and the a priori values), and determine the contribution of different input variables to the posterior estimates. These issues are addressed in Sect. 3.1.

3 Methodology

3.1 Model input

The Bayesian approach was applied to time series of three land cover types: maize, a vineyard and a forest, measured during intensive field campaigns (Sect. 3.2). Measured values of five variables are directly used as input for the model: R_n, G, T_a, and q_a. The model is constrained further by measured values of T_s and a priori estimates of g_a and g_s. After calculation of the posterior values for the latter three variables, the sensible and latent heat fluxes are calculated with Eqs. (2 and 3). Measured sensible and latent heat fluxes are used for validation only.

It is assumed that the meteorological input is accurately known (without uncertainty): for R_n, G, T_a, q_a measured values are used ($R_n = \tilde{R}_n$, etc.; the squiggly symbol is consistently used to indicate a measurement or a priori estimate). This implies that for these four variables, a priori and posterior values are equal to each other. In contrast, to the other variables, g_a, g_s and T_s, uncertainty is attributed.

HESSD
6, 2337–2365, 2009

The following equations for g_a, g_s and T_s are introduced:

$$\begin{aligned} g_a &= \theta_1 u = \left(\tilde{\theta}_1 + w_1\right) u \\ g_s &= \theta_2 = \tilde{\theta}_2 + w_2 \\ T_s &= \tilde{T}_s + w_3 \end{aligned} \tag{8}$$

where w indicates noise, θ_1 is a dimensionless parameter which includes the effects of surface roughness and stability of the boundary layer, u is wind speed (m s^{-1}), and parameter θ_2 is surface conductance (m s^{-1}). The a priori estimate for parameter θ_1 for neutral conditions is calculated using a logarithmic wind profile following Tennekes (1973) and Goudriaan (1977):

$$\tilde{\theta}_1 = \frac{\kappa^2}{\ln\left(\frac{z-d}{z_{0\mathrm{M}}}\right)\ln\left(\frac{z-d}{z_{0\mathrm{H}}}\right)} \tag{9}$$

where d=0.67h, $z_{0\mathrm{M}}$=0.13h, z_{0H}=0.1$z_{0\mathrm{M}}$, h is the vegetation height, z the measurement height of wind speed (all in m), and κ (=0.4) is Von Kármán's constant. Equation (9) does not include a correction term for non-neutral atmospheric conditions. For the a priori estimate of parameter θ_2, the FAO standard value for short, well watered grass of g_s=0.0143 is used for all three study sites. Values for $\tilde{T}_s$ are computed from Stefan-Boltzman equation, using measured outgoing longwave radiation and an emissivity of 0.98. For the forest site, no reliable measurements of outgoing longwave radiation were available. For this site, measured contact temperatures were used.

The issue is now to quantify the uncertainty of the a priori estimates and measurements, and their covariances. These determine the matrices C_x and C_t in Eq. (7).

It is assumed that the probability of θ_1, θ_2 and T_s have normal distributions with a standard deviation of one quarter of the difference between their upper and lower limits found in the literature. The upper and lower limit of θ_1 for crops (in this case maize and vineyard) and for forest are based on minimum and maximum values for $z_{0\mathrm{M}}$ reported in a review paper of Garratt (1993). For these extreme values of $z_{0\mathrm{M}}$, corresponding extreme crop heights ($h = z_{0M}/0.13$), zero plane displacement height (d=2/3h) and measurement height (z=h+2) are calculated. The upper and lower limits of θ_1 are calculated from the corresponding values of z_{0M}, z, h and d with Eq. (9). To estimate the upper and lower limits of θ_2 an empirical equation for g_s of Allen et al. (1998) is used:

$$g_s = \frac{LAI_{\text{active}}}{100} \tag{10}$$

where LAI_{active} is the leaf area index (m^2 leaf m^{-2} surface) that contributes to transpiration. For the upper and lower limits of θ_2 (i.e. g_s), the values corresponding to a LAI_{active} of respectively 3.5 and 0 are used. The upper and lower limit of T_s is estimated by applying Stefan-Boltzmann equation for two extreme values of emissivity (0.90 and 0.99 for the vineyard and 0.95 and 0.99 for the fully grown maize). For the forest site, the standard deviation of the readings of 9 thermocouples is used as a proxy for the standard deviation of T_s. Table 2 presents the a priori values and standard deviations $\sigma_{\theta 1}$, $\sigma_{\theta 2}$ and σ_{Ts} derived in this way.

It is further assumed that the covariances (cov(θ_1, θ_2), cov(θ_1, T_s), cov(θ_2,T_s)) are zero, and that the errors in θ_1, θ_2 and T_s of consecutive time steps of a time series are uncorrelated. The latter assumption may not be realistic: roughness estimates and surface temperature measurements may be biased and errors in θ_1 and T_s are therefore most likely similar for consecutive time steps. It appears however that reasonable results can be obtained even without using a Kalman filter for updating of a priori values. Assuming that all covariances are zero makes it possible to solve Eq. (7) for every time step individually. This is computationally more efficient than solving Eq. (7) for the whole time series at once, which requires manipulation of large matrices containing the parameters of all time steps.

The posterior parameters for an individual time step are now calculated with Eq. (7),

HESSD

6, 2337–2365, 2009

A Bayesian approach to estimate sensible and latent heat over vegetation

C. van der Tol et al.

using:

$$\boldsymbol{\theta} = \begin{pmatrix} \theta_1 \\ \theta_2 \end{pmatrix} \text{ and } \boldsymbol{\theta}_0 = \begin{pmatrix} \tilde{\theta}_1 \\ \tilde{\theta}_2 \end{pmatrix} \tag{11}$$

$$C_\theta = \begin{pmatrix} \sigma_{\theta 1}^2 & 0 \\ 0 & \sigma_{\theta 2}^2 \end{pmatrix} \text{ and } C_x = \sigma_{Ts}^2 \tag{12}$$

Negative values for the posterior parameter values are not allowed.

For comparison, sensible and latent heat fluxes are calculated using three methods, two of which have been presented in Sect. 2:

1. T_s-approach: using Eqs. (1–3) with H, λE and g_s as unknowns, and using the a priori expression for g$_a$ ($g_a = \tilde{\theta}_1 u$) and measured T_s. This method, albeit with a more sophisticated expression for g_a, is used in SEBS.

2. A priori approach: using Eqs. (1–3) with H, λE and T_s as unknowns, and using a priori values for g_a and g_s. This method, albeit with more sophisticated expressions for g_s, is commonly used in SVAT models.

3. Bayesian approach: using Eqs. (1–3) with H, λE and T_s as unknowns, and using posterior values for g_a and g_s, obtained from 7.

3.2 Experimental setup

The Bayesian approach is applied to three time series of different land cover and different environmental conditions: a maize crop (Sonning, UK), a vineyard (Barrax, Spain) and a Spruce forest (Speulderbos, The Netherlands). For the maize crop, 9 days, for the vineyard, 6 days and for the forest, 3.5 days worth of half-hourly data are used.

3.2.1 The maize field

Meteorological input variables and fluxes were obtained over a fully grown maize field (row spacing was 0.75 m, the within-row spacing was about 0.12 m) located at the

Crops Research Unit at Sonning farm (a research facility owned by the University of Reading, UK). It is located 4 km from Reading in Sonning (UK), at 51.48 N, 0.90 W, elevation 35 m above sea level (See Houldcroft, 2004); the soil type is loamy sand. Data from 7 to 16 September 2002 were used, when the leaf area index was 3.4 $m^2\,m^{-2}$ and the canopy height 1.9 m.

Net radiation was measured using a CNR1 four-component net radiometer (Kipp and Zonen, Delft, the Netherlands) at a mounting height of 2.5 m above the ground. Soil heat flux was calculated using a Fourier analysis on measured soil temperatures, combined with estimates of thermal diffusivity and heat capacity, the so-called analytical or exact method (see e.g. Verhoef, 2004). The soil temperatures were acquired with type-NT 10 kΩ thermistors (RS, UK) that had been encapsulated with a stainless steel housing, accuracy of ±0.2°C, installed at nominal depths of 2 and 5 cm. Soil heat flux at the surface (z=0), i.e. G, was calculated by using a negative z (i.e. −0.02 m) in the analytical equation of soil heat flux. Thermal diffusivity was calculated using the Arctangent method, using soil temperature signals at both depths, and heat capacity was calculated from the soil moisture content at 5 cm depth, measured using a Thetaprobe (Delta-T Devices).

Wind speed was measured using an AN1 cup anemometer (Delta-T Devices, UK), air temperature and humidity were measured with a RHT2 psychrometer, all at a height of 4 m above the vegetation. Surface temperature was estimated by inverting Stefan-Boltzmann's law, using outgoing longwave radiation measured with the CNR1 radiometer and an emissivity of 0.98. Although contact temperature measurements of the surface were available as well, these were not used in order to resemble remote sensing measurements as much as possible.

Sensible and latent heat fluxes were obtained using a combination of a Solent R3 sonic anemometer (Gill Instruments Ltd, Lymington, Hampshire, UK) and a differential closed-path infrared gas analyser (LI-7500, LICOR Inc., Lincoln, NE, USA).

3.2.2 The vineyard

Meteorological input variables and fluxes were obtained over vineyard (row spacing was 3.35 m, the within-row spacing was about 1.5 m, LAI was 0.52 $m^2 m^{-2}$, fractional vegetation cover 0.33 and vegetation height about 2 m) located at the Barrax agricultural test site in Spain (39.06 N, 02.10 W), where various crops were grown, some of them irrigated. Data were collected between 14 and 21 July 2004 during an intensive field campaign (SPARC). The experiment has been described in detail by Su et al. (2008).

Net radiation was measured using a CNR1 four-component net radiometer at a mounting height of 4.8 m above the ground. Soil heat flux was measured with 3 Hukseflux HFP01 heat flux plates (Campbell Scientific Inc., USA) at 0.5 cm depth. Heat storage above the sensors was neglected. Air temperature and relative humidity were measured with a HMP45 sensor (Vaisala, Finland) at 4.78 m height, wind speed with a cup anemometer (Vector Instruments, Ltd., United Kingdom) at 4.88 m height. Surface temperature was estimated by inverting Stefan-Boltzmann's law, using outgoing longwave radiation measured with the CNR1 radiometer and an emissivity of 0.98. All data were collected at 1 min interval, and 10-min averages were stored, and half hourly averages were used in this study.

Sensible and latent heat fluxes were obtained using a combination of a Solent R3 sonic anemometer (Gill Instruments Ltd, Lymington, Hampshire, UK) and a differential closed-path infrared gas analyser (LI-7500, LICOR Inc., Lincoln, NE, USA) at 3.4 m height. The representativeness of the flux measurements has been questioned due to the small fetch and due to extreme conditions caused by irrigation in adjacent fields in an otherwise dry environment, causing horizontal advection (Timmermans et al., 2009).

HESSD

6, 2337–2365, 2009

A Bayesian approach to estimate sensible and latent heat over vegetation

C. van der Tol et al.

3.2.3 The forest

Meteorological input variables and fluxes were obtained over a Douglas fir stand planted in 1962 in the Veluwe forest ridge in the Netherlands (52.50 N, 05.69 E). The research site is equipped with a 47 m high measurement tower maintained by the Dutch National Institute for Public Health and the Environment (RIVM). The tree density is 785 trees per hectare and the tree height 32 m. Leaf area index is approximately 5 m^2 m_{-2}. The topography is slightly undulating with height variations of 10 to 20 m within distances of 1 km. Data were collected between 10 and 21 June 2006 during an intensive field campaign (EAGLE). Details about the field campaign are described by Su et al. (2009).

The instrumentation at the forest site was similar to that at the vineyard. Net radiation was measured at a height of 35 m. Soil heat flux was measured with Hukseflux heat flux plates at 0.5 cm depth below the litter layer. Temperature, humidity and wind speed were measured at 35 m height. Because of an issue with the CNR1 radiometer (the temperature of the instrument was not correctly measured), the outgoing longwave radiation could not be used to estimate surface temperature. Instead, contact temperatures were measured with Negative Temperature Coefficient (NTC) sensors, 9 of which were attached to needles and branches and 8 to the soil. The average temperature of the 9 NTC's connected to the vegetation was used as an estimate of surface temperature. Because of the dense vegetation, the contribution of soil temperature was neglected. Contact temperature measurements were only available between 15 and 21 June 2006. Meteorological measurements were carried out and data stored at 1 min intervals. Half-hourly averages were used in this study.

Sensible and latent heat flux were measured with a CSAT3 sonic anemometer (Campbell Scientific, USA) and an open path infrared gas analyser (LI-7500, LICOR Inc., Lincoln, NE, USA) installed at 47 m height. The data were processed with the software package ECpack (http://www.met.wau.nl/projects/jep/index.html) and corrections were carried out according to Van Dijk et al. (2004).

4 Results

Figure 1 shows plots of a number of variables versus time, measured and calculated with the three above mentioned methods, for one example day with clear sky conditions for each of the three field sites. The plotted variables are the difference between surface and air temperature (T_s–T_a), the aerodynamic and surface conductance g_a and g_s, and the sensible and latent heat flux H and λE.

The a priori approach follows the a priori values for both g_a and g_s, without making use of the measurements of T_s–T_a. For the Barrax site, this results in much lower modelled than measured T_s–T_a. The T_s approach follows the a priori values for g_a and the measurements for T_s–T_a, irrespective the corresponding values for g_s. The modelled vales for g_s are often outside the range of values found in the literature. The Bayesian approach follows the measured values for T_s–T_a whenever this does not require an unacceptable deviation from the a priori values for the conductances g_a and g_s.

The posterior values of g_a and g_s reveal actual information about the surface. Posterior aerodynamic conductance g_a does not deviate much from a priori, but surface conductance g_s shows a clear pattern. The highest values of g_s are found in the late morning for the maize and the forest. In the afternoon, g_s decreases until a minimum at 19:00. Semi-empirical models often predict a decreasing g_s caused by stomatal closure during the afternoon. In such models, g_s is a function of vapour pressure deficit. A similar relationship between g_s and vapour pressure deficit is also visible in the posterior values for surface conductance, calculated with the Bayesian approach (Fig. 2). The difference with semi-empirical models is that this relationship is not imposed nor calibrated from measured λE. The a priori values g_s are constant during the day and equal for the three sites. The information about the diurnal cycle of g_s is obtained from the surface temperature measurements. The vineyard has low values for posteriorg_s. This can be attributed to the low vegetation cover (0.33).

During the night, both fluxes (R_n, G, H and λE) and gradients (q_s–q_a and T_s–T_a)

are relatively small. Small errors in absolute sense in fluxes and gradients may then propagate into the values of g_a and g_s, leading to unacceptable values if g_a and g_s were fitted to the fluxes. During the night, the absolute value of G is the largest term in the energy balance. Errors in G are relatively important, but these have not been incorporated in the model.

During the night, g_s returns to its a priori value. A closer look at the meteorological data during the night showed that $|q_s - q_a|$ is close to zero (not shown), and consequently λE is close to zero, and $T_s - T_a$ is relatively insensitive to the value of g_s. Because of the insensitivity to g_s, the model error (Eq. 7) can not be reduced by adjusting g_s, and posterior g_s remains at the a priori value.

Figure 1 also shows that the a priori approach and the Bayesian approach are unable to reproduce night time surface temperatures of the vineyard and the forest. During the night, stable, stratified air conditions are formed, in which the aerodynamic conductance strongly reduces (Massman and Lee, 2002). We do not find this strong reduction of g_a in the posterior values. The reason is that the chosen standard deviation for θ_1 ($\sigma_{\theta 1}$) is too low to include night time stable conditions: if $\sigma_{\theta 1}$ were increased, then posterior θ_1 during the night reduces zero, and measured night-time surface temperatures are reproduced (not shown). However, increasing $\sigma_{\theta 1}$ also causes large variability of θ_1 during the day, and the diurnal cycle of posterior g_s will then be incorporated by the posterior θ_1. For this reason, and because it is difficult to quantify the effect of stability on $\sigma_{\theta 1}$ in an objective way, stability effects were not incorporated into the value of $\sigma_{\theta 1}$.

Concerning the fluxes H and λE, the following is observed. The a priori approach performs well during the night and in the morning, but underestimates H and overestimates λE during the afternoon. This confirms the role of afternoon stomatal closure. The T_s approach performs well during the afternoon, but poorly during the night and in the morning. The values of the fluxes calculated with the Bayesian approach always vary between that of a priori and the T_s approach. Of the tree approaches, the Bayesian approach follows the measurements the closest. For all three sites, the Bayesian approach is closer to the a priori approach in the morning and closer to the T_s approach in the afternoon.

Figures 3–5 confirm that the Bayesian approach results in the most accurate predictions of H and λE. These figures show scatter plots of modelled versus measured fluxes of H and λE for the three methods for the entire data series, per site. For all three sites, the Bayesian approach results in the lowest root mean square error for the fluxes. The Bayesian approach reduces both the bias and the scatter compared to the other two approaches.

Both the T_s-approach and the Bayesian approach overestimate λE of the vineyard. This may be caused by a measurement error rather than a model error. The vineyard was relatively small and surrounded by bare land, stubble fields and irrigated crops, which contaminated the eddy covariance signal (Timmermans et al., 2009). The high measured λE values may be attributed to an adjacent irrigated maize field. A different problem with the measurements is apparent in the forest, where measured R_n was 10% higher than the sum of H, λE and G. Because the model forces energy balance closure (Eq. 1), it is possible that λE is overestimated, while H is not underestimated (Fig. 5).

5 Discussion and conclusion

In data assimilation, it is critical to quantify the uncertainty associated to parameters and measurements. This is not always possible for lack of data. A starting point is to identify sources of error. In this particular study, the uncertainties of aerodynamic and surface conductance are relevant.

Aerodynamic roughness parameter θ_1 (surface roughness) can vary in space and time for two different reasons: variations in surface roughness and variations in atmospheric stability. The first is the dominant cause of variations in space (at a specific time of a satellite overpass), whereas the second is the dominant cause of variations in time (at a specific field site). Similarly, surface conductance, θ_2 , can vary in space and time for two different reasons: variations in plant species, vegetation density and soil moisture content on the one hand and variations in the diurnal cycle of stomatal regulation on the other hand. Again, the first is the dominant cause of spatial variations, and the second of temporal variations.

In this study, no distinction was made between sources of error. High standard deviations are used for the two conductances in order to cover different errors, although the effect of stability on aerodynamic conductance during the night was not incorporated (see Sect. 4). As an alternative to the approach presented in this paper, posterior conductances were also calculated using an unknown bias for aerodynamic conductance for the whole time series, with standard deviation $\sigma_{\theta 1}$. This approach led to results similar to those presented in this paper, although the difference between a priori and posterior aerodynamic conductance was higher.

The simple Bayesian approach led to improved estimates of sensible and latent heat flux of maize, vineyard and forest compared to more classic approaches which use either measured surface temperature or a priori parameter values. Posterior estimates reveal the diurnal pattern of surface conductance during the day (stomatal regulation), without using measured fluxes as input.

Acknowledgements. This research was funded by the Netherlands Institute for Space Research (SRON), project number EO-071. The SPARC and EAGLE campaigns were carried out in the framework of the Earth Observation Envelope Program of the ESA, and were partly financed by the EU 6FP Project, SRON EO-071, and the ITC International Institute for Geo-Information Science and Earth Observation. The Sonning field campaign was funded by the Natural Environmental Research Council (NERC, UK) and a CASE award from the Environment Agency (EA, UK). We thank Bruce Main for his technical assistance in the field. The authors thank Jan Elbers, Wim Timmermans, Remco Dost, and Li Jia for fieldwork and data processing and coordination during the SPARC and EAGLE campaigns, and Wout Verhoef for fruitful discussion.

References

Allen, R. G., Pereira, L. S., Raes, D., and Smith, M.: Crop evapotranspiration. Guidelines for computing crop water requirements, FAO Irrigation and Drainage Paper (FAO) no. 56, Rome, Italy, 1998.

Allen, R. G., Pruitt, W. O., Wright, J. L., Howell, T. A., Ventura, F., Snyder, R., Itenfisu, D., Steduto, P. Berengena, J., Yrisarry, J. B., Smith, M., Pereira, L. S., Raes, D., Perrier, A., Alves, I., Walter, I., and Elliott, R.: A recommendation on standardized surface resistance for hourly calculation of reference ETo by the FAO56 Penman-Monteith method, Agr. Water Manage., 81(1–2), 1–22, 2006.

Baldocchi, D. D., Luxmoore, R. J., and Hatfield, J. L.: Discerning the forest from the trees: an essay on scaling canopy stomatal conductance, Agr. Forest Meteorol., 54, 197–226, 1991.

Ball, J., Woodrow, I., and Berry, J.: A model predicting stomatal conductance and its contribution to the control of photosynthesis under different environmental conditions, in: Progress in photosynthesis research, Martinus-Nijhoff, The Netherlands, 221–224, 1987.

Bastiaanssen, W. G. M., Menenti, M., Feddes, R. A., and Holtslag, A. A. M.: A remote sensing surface energy balance algorithm for land (SEBAL). 1. Formulation, J. Hydrol., 212–213, 198–212, 1998.

Cowan, I.: Stomatal behaviour and environment, Adv. Bot. Res., 4, 117–228, 1977.

Crow, W. T. and Wood, E. F.,: The assimilation of remotely sensed soil brightness temperature imagery into a land surface model using ensemble Kalman filtering: a case study based on ESTAR measurements during SGP97, Adv. Water Resour., 26(2), 137–149, 2003.

Franks, S. W., Beven, K. J., and Gash, J. H. C.: Multi-objective conditioning of a simple SVAT model, Hydrol. Earth Syst. Sci., 3(4), 477–489, 1999.

Garratt, J. R.: The Atmospheric Boundary Layer, Cambridge University Press, UK, 316 pp., 1992.

Garratt, J. R.: Sensitivity of climate simulations to land–surface and atmospheric boundary layer treatments – a review, J. Climate, 6, 419–449, 1993.

Goudriaan, J.: Crop micrometeorology: a simulation study. WAU dissertation no. 683, Wageningen University, The Netherlands, 249 pp., 1977.

Houldcroft, C.: Measuring and modeling the surface temperature and structure of a maize canopy, PhD Thesis, The University of Reading, UK, 235 pp., 2004.

Jarvis, P. O.: The interpretation of the variations in leaf water potential and stomatal conductance found in canopies in the field, Philos. T. Roy. Soc. B., 273, 593–610, 1976.

Leuning, R.: A critical appraisal of a combined stomatal-photoynthesis model for C3 plants, Plant Cell Environ., 18, 339–355, 1995.

Massman, W. J. and Lee, X.: Eddy covariance flux corrections and uncertainties in long-term studies of carbon and energy exchanges, Agr. Forest Meteorol. 113(1–4), 121–144, doi:10.1016/S0168-1923(02)00105-3., 2002.

Raupach, M. R.: Simplified expressions for vegetation roughness length and zero-plane displacement as functions of canopy height and area index, Bound. Lay. Meteorol., 71, 211–216, 1994.

Reichle, R. H., McLaughlin, D. B., and Entekhabi, D.: Hydrologic Data Assimilation with the Ensemble Kalman Filter, Mon. Weather Rev., 130, 103–114, 2002.

Schuurmans, J. M., Troch, P. A., Veldhuizen, A. A., Bastiaanssen, W. G. M., and Bierkens, M. F. P.: Assimilation of remotely sensed latent heat flux in a distributed hydrological model, Adv. Water Resour., 26, 151–159, 2007.

Stewart, J. B., Kustas, W. P., Humes, K. S., Nichols, W. D., Moran, M. S., and De Bruin, H. A. R.: Sensible Heat Flux-Radiometric Surface Temperature Relationship for Eight Semiarid Areas, J. Appl. Meteorol., 33(8), 1110–1117, 1994.

Su, Z.: The surface energy balance system (SEBS) for estimation of turbulent heat fluxes, Hydrol. Earth Syst. Sci., 6(1), 85–99, 2002.

Su, Z., Timmermans, W., Gieske, A., Jia, L., Elbers, J. A., Olioso, A., Timmermans, J., Van Der Velde, R., Jin, X., Van Der Kwast, H., Nerry, F., Sabol, D., Sobrino, J. A., Moreno, J., and Bianchi, R.: Quantification of land-atmosphere exchanges of water, energy and carbon dioxide in space and time over the heterogeneous Barrax site, Int. J. Remote Sens., 29, 5215–5235, doi:10.1080/01431160802326099, 2008.

Su, Z., Timmermans, W. J., Van der Tol, C., Dost, R., Bianchi, R., Gómez, J. A., House, A., Hajnsek, I., Menenti, M., Magliulo, V., Esposito, M., Haarbrink, R., Bosveld, F., Rothe, R., Baltink, H. K., Vekerdy, Z., Sobrino, J. A., Timmermans, J., Van Laake, P., Salama, S., Van der Kwast, H., Claassen, E., Stolk, A., Jia, L., Moors, E., Hartogensis, O., and Gillespie, A.: EAGLE 2006 – Multi-purpose, multi-angle and multi-sensor in-situ and airborne campaigns over grassland and forest, Hydrol. Earth Syst. Sci., in review, 2009.

Tennekes, H.: The Logarithmic Wind Profile, J. Atmos. Sci., 30(2), 234–238, 1973.

Timmermans, W. J., Su, Z., and Alioso. A.: Footprint issues in scintillometry over a heterogeneous landscape, Hydrol. Earth Syst. Sci., in review, 2009.

Troch, P. A., Paniconi, C., and McLaughlin, D. B.: Catchment- scale hydrological modeling and data assimilation, Adv. Water Resour., 26, 131–217, 2003.
Van Dijk, A., Moene, A. F., and De Bruin, H. A. R.: The principles of surface flux physics: theory, practice and description of the ECPACK library, Internal Report 2004/1, Meteorology and Air Quality Group, Wageningen University, Wageningen, The Netherlands, 99 pp., 2004.
Verhoef, A.:. Remote estimation of thermal inertia and soil heat flux for bare soil, Agr. Forest Meteorol., 123(3–4), 221–236, 2004.
Verhoef, A. and Campbell, C. L.: Evaporation Measurement, Ch. 40, in: Encyclopedia of Hydrological Sciences, edited by: Anderson, M. G., John Wiley, Chichester, UK, 589–601, 2005.
Verhoef, A., McNaughton, K. G., and Jacobs, A. F. G.: A parameterization of momentum roughness length and displacement height for a wide range of canopy densities. Hydrol. Earth Syst. Sci., 1(1), 81–91, 1997a.
Verhoef, A., De Bruin, H. A. R., and Van den Hurk, B. J. J. M.: Some practical notes on the parameter kB^{-1} for sparse canopies. J. Appl. Meteorol., 36, 560–572, 1997b.

Table 1. Unknowns in the energy balance equations (Eqs. 1–3).

Description	Symbols	Units
Energy balance terms	R_n, G, H, λE	$\mathrm{W\,m^{-2}}$
Conductances	g_a, g_s	$\mathrm{m\,s^{-1}}$
Air and surface temperature	T_a, T_s	K
Vapour concentration in the air and in soil and leaf pores	q_a, q_s	$\mathrm{kg\,m^{-3}}$

HESSD

6, 2337–2365, 2009

Table 2. A priori values for θ_1 and θ_2, and standard deviations for θ_1, θ_2 and T_s.

	σT_s (K)	$\theta_1 \times 10^3$ (–)	$\sigma_{\theta 1} \times 10^3$ (–)	$\theta_2 \times 10^3$ (mm s^{-1})	$\sigma_{\theta 2} \times 10^3$ (mm s^{-1})
Sonning (maize)	0.74	9.8	3.6	14.3	8.8
Barrax (vineyard)	2.47	5.7	3.6	14.3	8.8
Speulderbos (forest)	1.37	44.6	14.2	14.3	8.8

HESSD

6, 2337–2365, 2009

A Bayesian approach to estimate sensible and latent heat over vegetation

C. van der Tol et al.

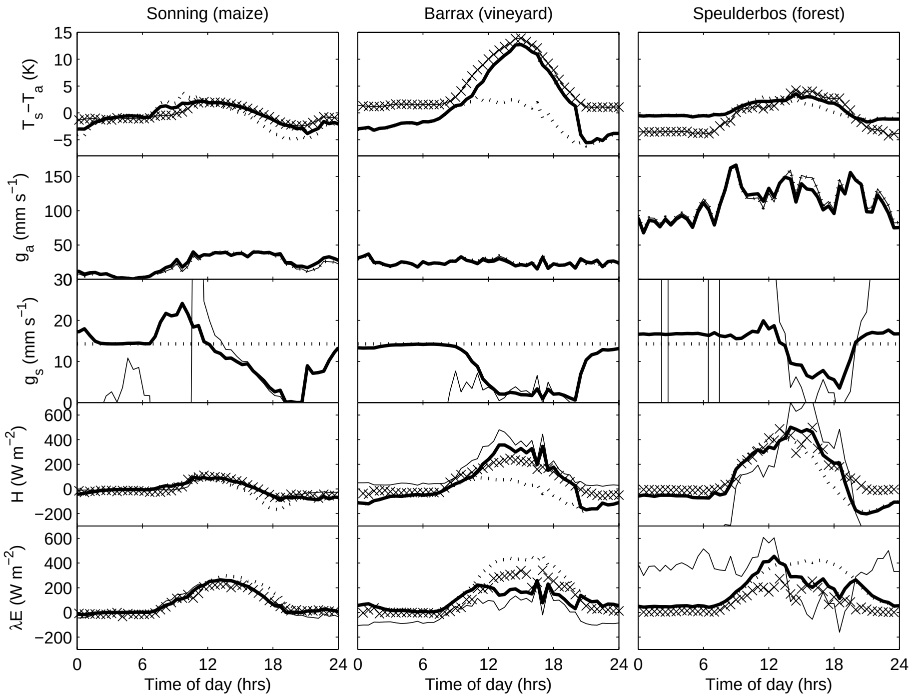

Fig. 1. Measured and modelled values of (T_s – T_a), aerodynamic conductance g_a, surface conductance g_s, sensible heat flux H, and latent heat flux λE versus time. The data represent example days for a fully-grown maize field in Sonning (UK) on 13 September 2002, a vineyard in Barrax (Spain) on 15 July 2004, and a forest in Speulderbos (the Netherlands) on 16 June 2006. The dashed line represents the a priori approach, the thin solid line the T_s approach, the bold solid line the Bayesian approach, and the symbol "x" represents a field measurement.

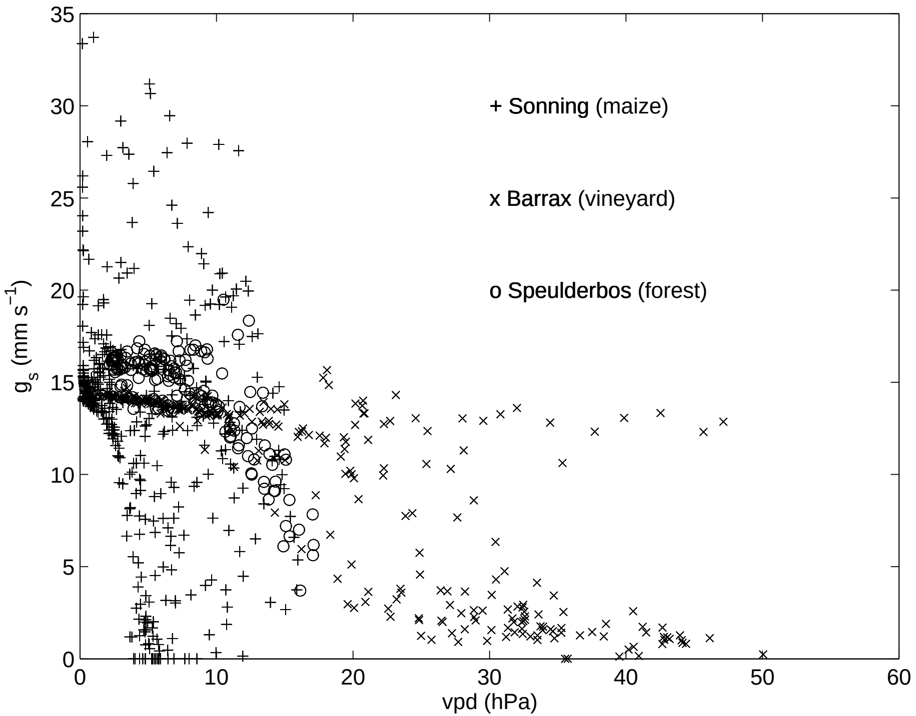

Fig. 2. Scatter plot of posterior surface conductance versus atmospheric vapour pressure deficit for all half-hourly data of the three sites.

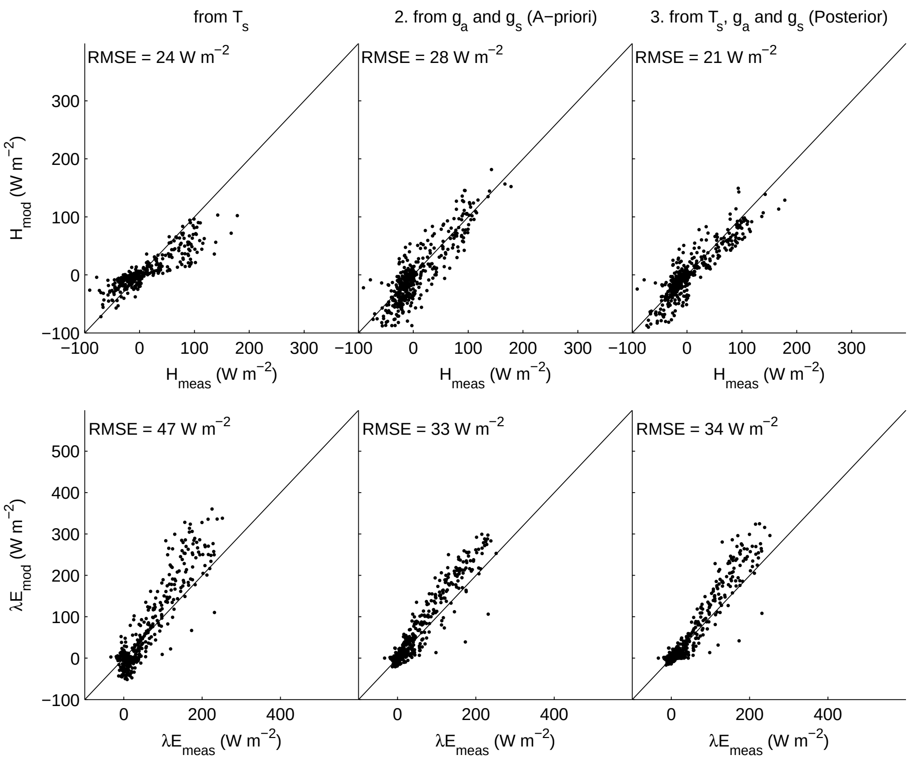

Fig. 3. For the maize field (Sonning), for all half-hourly data in the measurement period, modelled versus measured sensible heat flux H (upper graphs) and latent heat flux λE (lower graphs), for the a priori approach (left), the T_s-approach (middle) and the Bayesian approach (right).

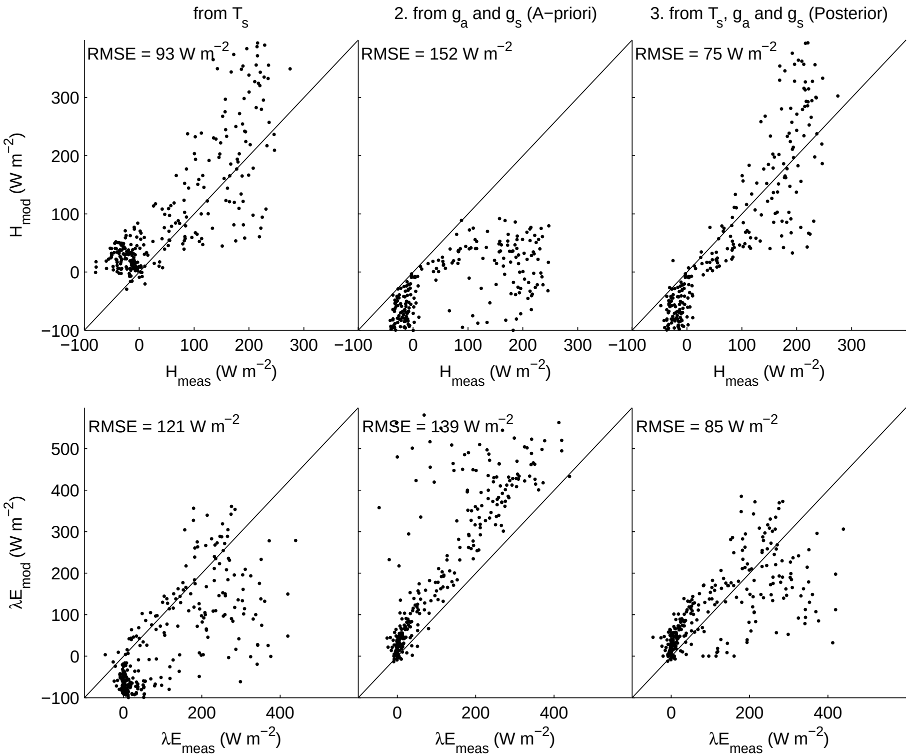

Fig. 4. Similar to Fig. 2, but for the vineyard (Barrax).

HESSD

6, 2337–2365, 2009

A Bayesian approach to estimate sensible and latent heat over vegetation

C. van der Tol et al.

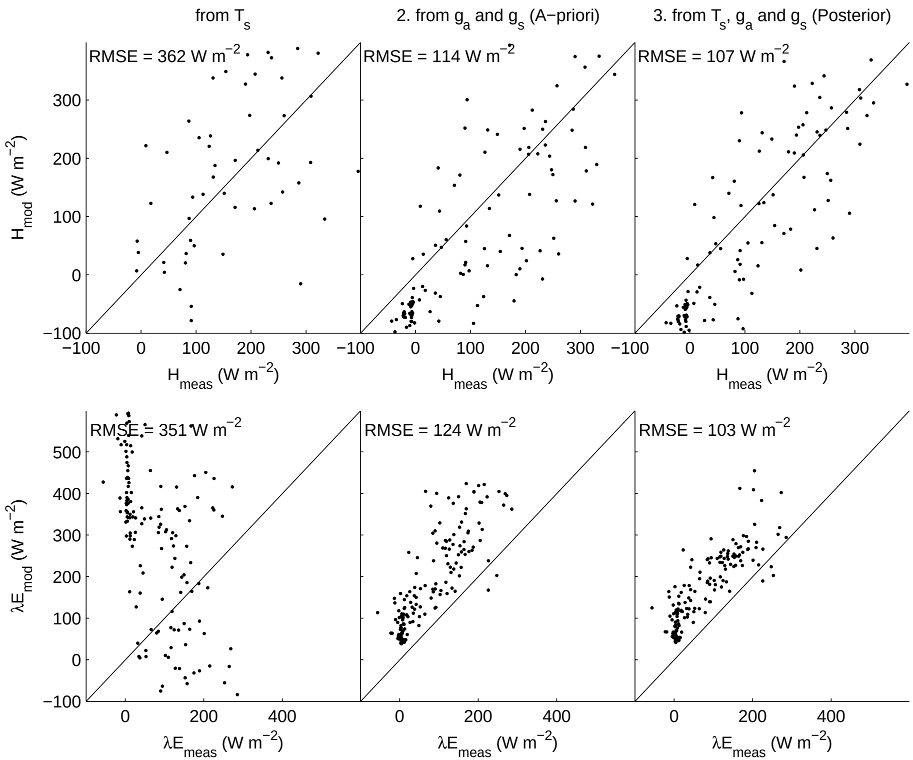

Fig. 5. Similar to Fig. 2, but for the forest (Speulderbos).

HESSD
6, 2337–2365, 2009

A Bayesian approach to estimate sensible and latent heat over vegetation

C. van der Tol et al.